December 1984:1213–21

Stress Thallium-201 Transaxial Emission Computed Tomography: Quantitative Versus Qualitative Analysis for Evaluation of Coronary Artery Disease

NAGARA TAMAKI, MD, YOSHIHARU YONEKURA, MD, TAKAO MUKAI, PHD, SHUSEI KODAMA, MD, KAZUNORI KADOTA, MD,* HIROFUMI KAMBARA, MD,* CHUICHI KAWAI, MD, FACC,* KANJI TORIZUKA, MD

Kyoto, Japan

Stress thallium-201 myocardial distribution was quantitatively evaluated by emission transaxial tomography in 104 patients who underwent coronary arteriography. The initial uptake and percent washout of thallium were assessed by the circumferential profile curves of the three short-axis sections and one middle right anterior oblique long-axis section. This quantitative tomographic analysis showed abnormal distribution in all but two patients (98%) with coronary artery disease, whereas qualitative analysis showed abnormality in 76 of the patients (93%).

Quantitative analysis showed better sensitivity (91%) for detecting involved coronary vessels than qualitative analysis (80%, $p < 0.01$), especially in three vessel disease (82 versus 67%, $p < 0.05$). For localization of individual vessel involvement, quantitative analysis showed high sensitivity (right coronary artery: 96%, left anterior descending artery: 90% and left circumflex artery: 88%) as compared with qualitative analysis (88, 83 and 63%, respectively, $p < 0.05$), while similar specificity was observed (92% for quantitative and 93% for qualitative analyses). Furthermore, in the study of patients without infarction, myocardial segments supplied by coronary vessels with moderate stenosis (51 to 75%) revealed abnormality more often with quantitative (81%) than with qualitative (56%) analysis.

Thus, quantitative analysis of stress thallium emission tomography provides improved sensitivity for the detection of diseased coronary vessels in patients with three vessel disease and those with moderate stenosis. It is a valuable technique for the evaluation of coronary artery disease.

Thallium-201 myocardial imaging has been widely used in the diagnosis of coronary artery disease (1–5). However, when thallium myocardial scintigrams are interpreted visually, considerable interobserver variability is inevitable because of normal variation in thallium distribution (5). To solve this problem, several methods of quantitative analysis of thallium distribution have been described (6–11). However, these techniques have not significantly improved diagnostic accuracy for the detection of coronary artery disease as compared with visual interpretation (6–11). One of the major limitations of this technique is two-dimensional expression of thallium distribution in the myocardium.

Since Holman et al. (12) emphasized the diagnostic value of thallium emission computed tomography, we (13) and other investigators (14,15) have reported improved sensitivity of thallium emission tomography for diagnosing prior myocardial infarction compared with the conventional planar technique. However, only limited data have described the value of stress emission tomography for diagnosing coronary artery disease and identifying individual vessel involvement (16,17). Maddahi et al. (11) suggested improved sensitivity by identifying ischemic zones using thallium washout curve analysis from planar imaging. This study was undertaken to determine whether stress emission tomography provides high diagnostic accuracy and whether thallium uptake and washout analysis using emission tomography further improves accuracy as compared with qualitative analysis.

Methods

Patient selection. The study group consisted of 104 consecutive patients who were referred to our hospital for evaluation of chest pain by coronary arteriography. Eighty-two patients had significant coronary artery disease (> 50%

From the Department of Radiology and Nuclear Medicine, and *The Third Division, Department of Internal Medicine, Kyoto University School of Medicine, Kyoto, Japan. Manuscript received February 21, 1984; revised manuscript received May 22, 1984, accepted June 12, 1984.

Address for reprints: Nagara Tamaki, MD, Department of Radiology and Nuclear Medicine, Kyoto University School of Medicine, Sakyo-ku, Kyoto 606, Japan.

0735-1097/84/$3.00

JACC Vol. 4, No. 6
December 1984:1213–21

diameter narrowing), of whom 32 had one or more previously documented myocardial infarctions confirmed by a typical history and enzymatic and electrocardiographic alterations. The remaining 22 patients had no or minor coronary stenosis (< 25% diameter narrowing) on angiography.

No patient had concomitant congenital, valvular or cardiomyopathic heart disease. All patients gave informed written consent.

Cardiac catheterization. Left ventriculography and selective coronary arteriography in multiple views were obtained in all patients. Coronary angiograms were projected on a screen, and the diameters of the pre- or poststenotic segments were measured as well as the stenotic segment by three experienced observers without knowledge of the thallium imaging or electrocardiographic findings. Narrowing in one or more major vessels was graded according to the lumen diameter involved: 25% or less, 26 to 50%, 51 to 75%, 76 to 90%, 91 to 99% or 100%. A significant narrowing was defined as more than 50% diameter stenosis.

Exercise protocol. The exercise test was performed using an upright bicycle ergometer with a graded work load starting at 25 watts and increasing after every 3 minute stage by an additional 25 watts. Each patient exercised to 85% of the age-predicted maximal heart rate or the onset of angina pectoris, dyspnea or fatigue, dizziness, frequent (> 10/min) multifocal or paired ventricular extrasystoles, ST segment depression (> 0.2 mV) or decrease in blood pressure of 10 mm Hg below the peak value of the previous stage.

Two millicuries of thallium-201 was injected intravenously through the indwelling cannula approximately 60 seconds before completion of exercise.

Tomographic acquisition. Tomographic acquisition started approximately 10 minutes (stress phase) and 2.5 hours (redistribution phase) after thallium injection. A small marker was placed on the anterior chest wall and the patient was positioned in exactly the same position on the repeat study by adjusting the marker activity on the same spot on the patient monitor.

Data collection was performed using a rotatable gamma camera (400 T, General Electric) with a low energy general purpose collimator interfaced to a digital computer (PDP 11/60, Digital Equipment Corp.). The camera was rotated with every 5.6° of revolution from 135° left posterior oblique position to the 45° right anterior oblique position of the patient, collecting 32 views over the anterior half (180°) of the heart (13,18). Each image was acquired for 30 seconds for a total acquisition time of approximately 16 minutes. System resolution in reconstructed images measured with a cylindrical phantom filled with water was 17 mm in full width-half maximum (18).

Image processing. A series of contiguous transverse tomograms of the left ventricular myocardium was reconstructed by a filtered back projection method using a convolution algorithm without attenuation correction (13,18). These images were further processed to obtain oblique tomograms: short-axis and right anterior oblique long-axis sections in two orthogonal perspectives aligned with respect to the cardiac axes as previously described (19,20). Cardiac axes were determined visually from the middle transverse section and middle long-axis section. Multiple sections (12 mm thick) were obtained contiguously in each tomographic plane. Each reconstructed slice contained 150,000 to 250,000 counts.

Qualitative analysis. The tomographic images were analyzed visually by two experienced observers who were unaware of the clinical diagnosis or coronary arteriographic findings. Enhanced digital images were used for visual interpretation of the tomographic images by subtracting 30 to 40% of the background as described previously (13).

Quantitative analysis. For quantitative tomographic analysis, the three central short-axis sections of the left ventricle with a doughnut configuration (apical, middle and basal sections) were selected. To assess the apical region,

Figure 1. Schematic presentation of three short-axis sections and one most central right anterior oblique long-axis section of the left ventricular myocardium and the distribution of the three major coronary arteries. Each emission computed tomographic (ECT) image was divided into 36 radial segments to create a circumferential maximal count profile curve. LAD = left anterior descending artery; LCx = left circumflex artery; RCA = right coronary artery.

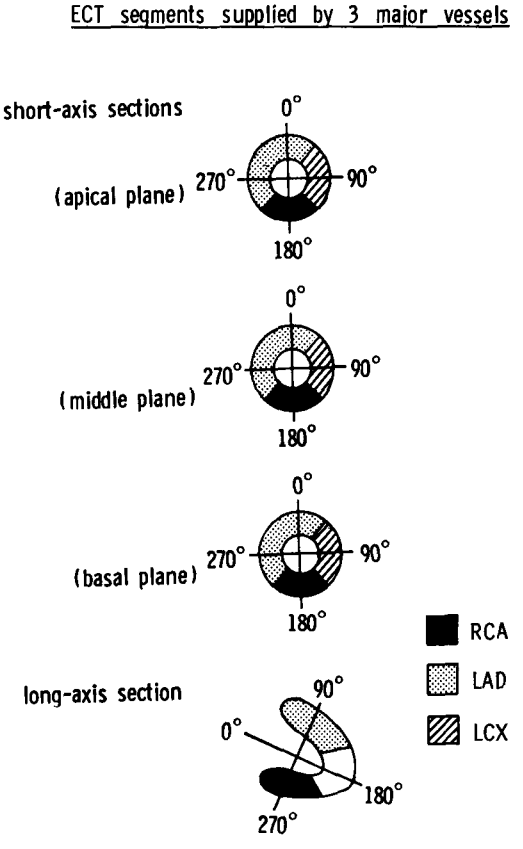

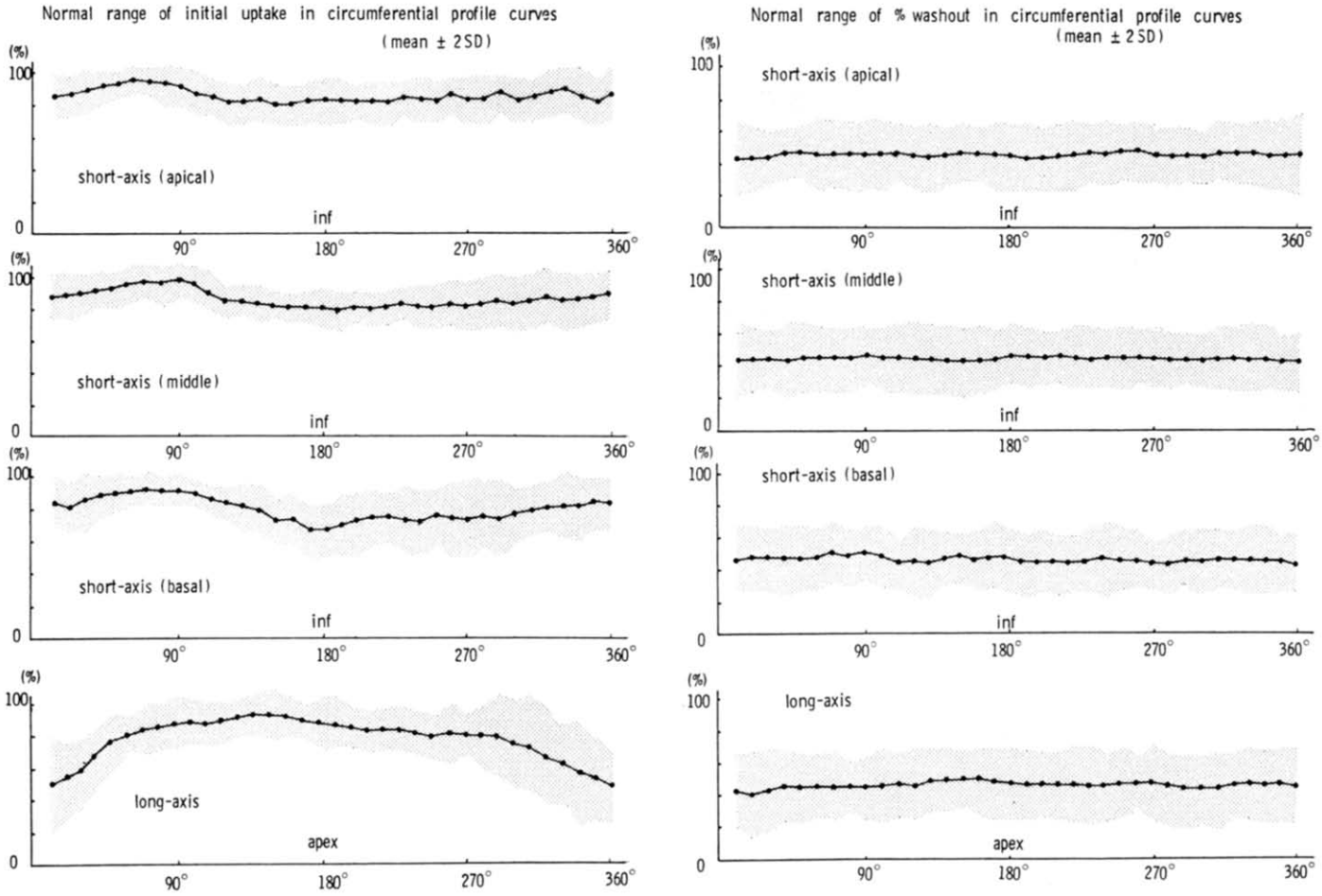

Figure 2. Normal range profile curves of initial thallium uptake (**left**) and percent washout (**right**). The **middle curves** indicate the mean values and the upper and lower limits are shown by the mean ± 2 standard deviation curves. inf = inferior.

the most central long-axis section cutting through the apex was also selected.

Distribution profiles. From these images, circumferential maximal count profiles of myocardial distribution were obtained in a manner similar to that of Meade (6) and Burow (7) and their coworkers. The center of the left ventricular cavity was manually determined, and each tomographic image was divided into 36 radial segments at 10° intervals. The distribution of thallium activity was determined by calculating the highest activity per pixel along each radial segment, normalizing the data to the segment with the highest counts to display a circumferential profile curve in each image (7). The highest counts in each radial segment were 150 to 250 counts. In the short-axis sections, the profile started at the 12 o'clock position proceeding clockwise. In the long-axis section, the apex was used as a landmark (180°) to align circumferential profiles (Fig. 1).

Washout rate profiles. In addition to the distribution profiles, washout rate circumferential profiles (WRP) were generated as percent washout from stress for the 2.5 hour intervals in each section according to the equation:

$$\%\text{WRP}\ (\theta) = \frac{\text{p}\ (\theta\ \text{EX}) - \text{p}\ (\theta\ \text{RD})}{\text{p}\ (\theta\ \text{EX})} \times 100\ (\%),$$

Table 1. Overall Sensitivity and Specificity of Stress Thallium Emission Tomography for Diagnosing Coronary Artery Disease*

	Visual	Initial Uptake	Uptake and Washout
Sensitivity			
No infarction	45 of 50 (90%)	48 of 50 (96%)	48 of 50 (96%)
Overall	76 of 82 (93%)	80 of 82 (98%)	80 of 82 (98%)
Specificity	20 of 22 (91%)	20 of 22 (91%)	20 of 22 (91%)

*The values indicate the number and percent of patients with coronary artery disease studied.

JACC Vol. 4, No. 6
December 1984:1213–21

Table 2. Sensitivity for Detecting Coronary Vessel Involvement in Relation to the Number of Diseased Vessels on Angiography

	All Patients With CAD (n = 73)		
	Visual	Uptake	Uptake and Washout
1VD	36 of 40 (90%)	39 of 40 (98%)	39 of 40 (98%)
2VD	39 of 44 (89%)	41 of 44 (93%)	43 of 44 (98%)
3VD	40 of 60 (67%)	45 of 60 (75%)	49 of 60 (82%)*
Total	115 of 144 (80%)	122 of 144 (87%)	131 of 144 (91%)†
	Patients Without Infarction (n = 41)		
	Visual	Uptake	Uptake and Washout
1VD	21 of 24 (88%)	23 of 24 (96%)	23 of 24 (96%)
2VD	25 of 28 (89%)	26 of 28 (93%)	28 of 28 (100%)
3VD	24 of 36 (67%)	25 of 36 (69%)	27 of 36 (75%)
Total	69 of 88 (78%)	74 of 88 (84%)	78 of 88 (89%)

*$p < 0.05$ compared with the visual analysis. †$p < 0.01$ compared with the visual analysis. CAD = coronary artery disease; VD = vessel disease.

where %WRP (θ) is the washout from a myocardial segment at the 2.5 hour redistribution phase and p (θ EX) and p (θ RD) represent maximal count profiles in the segment in the exercise and redistribution phases, respectively.

Normal limits were defined as the curves representing 2 standard deviations below the mean value derived from the distribution and washout profiles of 12 previously studied normal cases.

Interpretation. From segmental analysis of stress emission tomography, a perfusion abnormality in the inferior and posterior walls was defined as a right coronary artery (or posterior descending artery) lesion, that in the septal and anterior walls as a left anterior descending lesion and that in the posterolateral wall as a left circumflex lesion (Fig. 1) (16,21). In the short-axis section profiles, 45 to 135° segments were defined as left circumflex area, 135 to 225° segments as right coronary area and 225 to 45° segments as left anterior descending area. In the long-axis section profile, 45 to 150° segments were defined as left anterior descending area and 210 to 315° were defined as right coronary area. For quantitative interpretation, the patient profiles in which two or more 10° contiguous radial segments fell below normal limits were considered abnormal. In patients with left circumflex dominant or balanced coronary distribution, the posterior descending artery was considered to belong to the right coronary artery.

Abnormal perfusion was evaluated in the 104 cases regarding the following criteria: 1) segmental hypoperfusion judged by visual inspection; 2) initial distribution profiles below the normal limits; and 3) initial distribution or washout profiles below the normal limits.

Statistical analysis. Sensitivity was defined as the number of true positive tests × 100 ÷ the sum of true positive and false negative tests. Specificity was defined as the number of true negative tests × 100 ÷ the sum of true negative and false positive tests. The chi-square test with or without Yates' correction was used to determine the significance of a difference in observed rates of occurrence. A significant

Table 3. Sensitivity for Detecting Disease of the Three Major Coronary Vessels

	All Patients With CAD (n = 73)		
	Visual	Uptake	Uptake and Washout
RCA	43 of 49 (88%)	45 of 49 (92%)	46 of 49 (94%)
LAD	52 of 63 (83%)	55 of 63 (87%)	57 of 63 (90%)
LCx	20 of 32 (63%)	25 of 32 (78%)	28 of 32 (88%)*
	Patients Without Infarction (n = 41)		
	Visual	Uptake	Uptake and Washout
RCA	28 of 31 (90%)	28 of 31 (90%)	28 of 31 (90%)
LAD	30 of 38 (79%)	32 of 38 (84%)	34 of 38 (89%)
LCx	12 of 19 (63%)	14 of 19 (74%)	16 of 19 (84%)

*$p < 0.05$ compared with the visual analysis. CAD = coronary artery disease; LAD = left anterior descending artery; LCx = left circumflex artery; RCA = right coronary artery.

Table 4. Specificity for Detecting Absence of Disease of the Three Major Coronary Vessels

	Visual	Uptake	Uptake and Washout
RCA	49 of 55 (89%)	51 of 55 (93%)	50 of 55 (91%)
LAD	39 of 41 (95%)	40 of 41 (98%)	38 of 41 (93%)
LCx	69 of 72 (96%)	69 of 72 (96%)	66 of 72 (91%)
Total	157 of 168 (93%)	160 of 168 (95%)	154 of 168 (92%)

Abbreviations as in Table 3.

difference was considered to exist when a probability (p) value of 0.05 or less was observed.

Results

Normal range of the profiles. The mean curves of initial uptake (Fig. 2, left) and percent washout (Fig. 2, right) in the tomographic sections derived from the 12 previously studied normal cases are presented. The initial uptake was relatively high in the posterolateral regions (approximately 90° in profiles), although it was relatively low in the inferior and septal regions in middle and basal short-axis sections (180 to 270° in profiles) as well as in the inferoposterior regions in the long-axis sections (180 to 270° in profiles).

The percent washout was nearly constant in all segments in each tomographic section. The mean value (± standard deviation) was 48.4 ± 9.7%.

Interobserver variance in visual analysis. Disagreement between the two observers in subjective visual segmental analysis occurred in 2 (1.9%) of the 104 patients and in 26 (7.4%) of the 312 coronary vessels.

Sensitivity and specificity for diagnosing coronary disease. Overall sensitivity and specificity of the three tomographic analyses for diagnosing coronary artery disease are summarized in Table 1. Two of the 22 patients without significant coronary artery disease manifested an abnormality by each analysis, yielding a specificity of 91%.

Among the 82 patients with significant coronary artery disease, visual tomographic analysis showed abnormal perfusion in 76 patients (93%), whereas quantitative analysis showed abnormality in 80 patients (98%). Qualitative and quantitative analyses yielded a high sensitivity for detecting patients without prior infarction as well (90 and 96%, respectively).

Assessment of coronary vessel involvement. Table 2 summarizes the sensitivity of stress emission tomography for detecting coronary vessel involvement in relation to the number of diseased vessels. The quantitative analysis detected all but one diseased coronary vessel in patients with one vessel disease (98%) and more than 90% of the diseased vessels in patients with two vessel disease. In patients with three vessel disease, in contrast to relatively poor sensitivity (67%) by the qualitative analysis, the quantitative analysis improved the sensitivity to 82% ($p < 0.05$). Overall sensitivity was significantly higher by the quantitative uptake and washout analysis (91%) than by the visual analysis (80%, $p < 0.01$).

When the same study was limited to 50 patients without prior myocardial infarction, the sensitivity for detecting diseased coronary vessels was 89% by the quantitative uptake and washout analysis (96% in one vessel, 100% in two vessel and 75% in three vessel disease). These values were similar to those from all the study patients with coronary artery disease.

The sensitivity of stress emission tomography for detecting disease of the three major coronary arteries is listed in Table 3. The visual analysis detected most of the right coronary (88%) and left anterior descending (83%) lesions, but only 63% of the left circumflex lesions were recognized. The uptake and washout analysis also provided a high sensitivity in detecting right coronary and left anterior descending lesions (94 and 90%, respectively), and it improved the sensitivity for left circumflex lesions (88%, $p < 0.05$) as compared with the visual analysis. In the study of patients without prior myocardial infarction, similar results were observed.

The specificity for the detection of the absence of disease in individual vessels is listed in Table 4. Fourteen coronary vessels were falsely considered abnormal by the quantitative uptake and washout analysis, yielding a specificity of 92%. This was not statistically different from that of the qualitative and quantitative uptake analyses (93 and 95%, respectively).

Table 5. Sensitivity for Detecting Coronary Vessel Involvement in Relation to Severity of Stenosis in Patients Without Infarction

Diameter Stenosis	Overall (n = 88)			One Vessel Disease (n = 21)		
	Visual	Uptake	Uptake and Washout	Visual	Uptake	Uptake and Washout
51 to 75%	9 of 16 (56%)	13 of 16 (81%)	13 of 16 (81%)	4 of 7 (57%)	6 of 7 (86%)	6 of 7 (86%)
76 to 90%	32 of 37 (86%)	32 of 37 (86%)	34 of 37 (92%)	11 of 11 (100%)	11 of 11 (100%)	11 of 11 (100%)
91 to 100%	29 of 35 (83%)	29 of 35 (83%)	31 of 35 (89%)	3 of 3 (100%)	3 of 3 (100%)	3 of 3 (100%)

JACC Vol. 4, No. 6
December 1984:1213-21

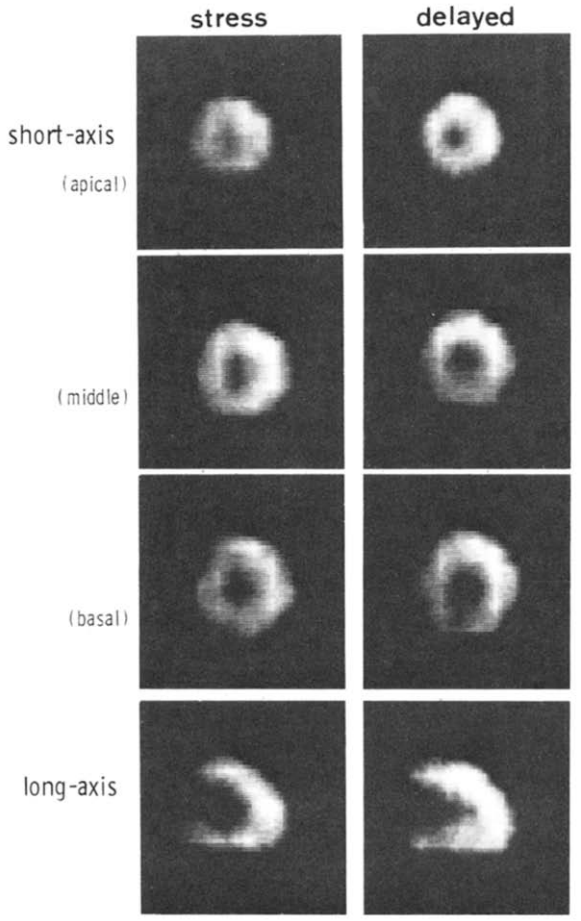

Figure 3. Stress (**left**) and delayed (**right**) thallium emission tomographic images of a patient with coronary artery disease. Equivocal hypoperfusion is observed in the septal region, but no definite perfusion defect is noted.

Sensitivity relative to severity of narrowing. Table 5 lists the sensitivity for detecting coronary vessel involvement in relation to the severity of narrowing in the 50 patients without prior myocardial infarction. Abnormal perfusion was seen in most of the coronary vessels with more than 90% diameter stenosis (83% by visual analysis and 89% by uptake and washout analysis). In 16 coronary vessels with moderate stenosis (51 to 75% diameter stenosis), quantitative analysis detected 13 diseased coronary vessels (81%), whereas visual analysis detected only 9 (56%). In cases of one vessel disease in patients without prior myocardial infarction, six of seven coronary vessels with moderate stenosis (86%) were detected by quantitative analysis, whereas only four (57%) were recognized by visual analysis.

Representative case. Figure 3 shows representative stress and delayed tomographic images in a case of coronary artery disease without evidence of myocardial infarction. The coronary angiogram showed 70% stenosis in the proximal portion of the left anterior descending artery. The images revealed equivocal hypoperfusion in the septal region, but no significant perfusion defect. The initial uptake profile curves (Fig. 4) revealed low uptake in the septal wall in the apical and middle short-axis sections, indicating left anterior descending involvement. The percent washout curves showed delayed washout in the same region.

Discussion

Value of stress emission tomography. The results of this study show that thallium stress emission tomography yields high sensitivity and specificity for the detection of coronary artery disease and individual vessel involvement. Moreover, quantitative tomographic analysis further improved the sensitivity, especially in the study of multivessel disease and vessels with moderate stenosis.

The advantages of thallium emission tomography at rest in the evaluation of myocardial infarction have been described previously by us (13,21) and other investigators (12,14,15). Several preliminary reports (16,17,22) describe a high diagnostic performance of stress emission tomography. Our present results are consistent with preliminary data.

Stress planar imaging also yielded a high diagnostic accuracy for detecting coronary artery disease (1,2). However, it showed a rather poor sensitivity for the detection of individual vessel involvement. Massie et al. (23) reported that 98 (66%) of 148 diseased vessels were detected (right coronary artery: 73%, left anterior descending artery: 78%, left circumflex artery: 45%). Rigo et al. (24) reported similar but somewhat poorer results (50, 63 and 21%, respectively; 49% overall). Our results of stress planar imaging in our preliminary report (16) are consistent with previous reports (55, 70 and 36%, respectively; 57% overall).

Several factors may be responsible for the improved sensitivity of stress emission tomography for detecting diseased coronary vessels. 1) The full three-dimensional tomographic representation of thallium myocardial distribution overcomes the limitation imposed by planar imaging. Therefore, segmental analysis can be done more accurately (16). 2) Deep myocardial regions can be visualized better by tomographic expression. In our preliminary report (16), abnormal perfusion in the inferior and posterolateral walls was shown clearly so that a better diagnostic accuracy for detecting diseased right coronary and left circumflex coronary arteries was obtained by stress tomography than by planar imaging. 3) Because of high contrast images, tomography may detect a region of lesser ischemia as a hypoperfused area. 4) Increased thallium uptake in the lung that is occasionally seen in multivessel disease (25) may possibly impair precise assessment of thallium myocardial distribution by planar imaging. On the contrary, tomography can separate thallium myocardial distribution from the lung and abdominal activities. Consequently, qualitative and quan-

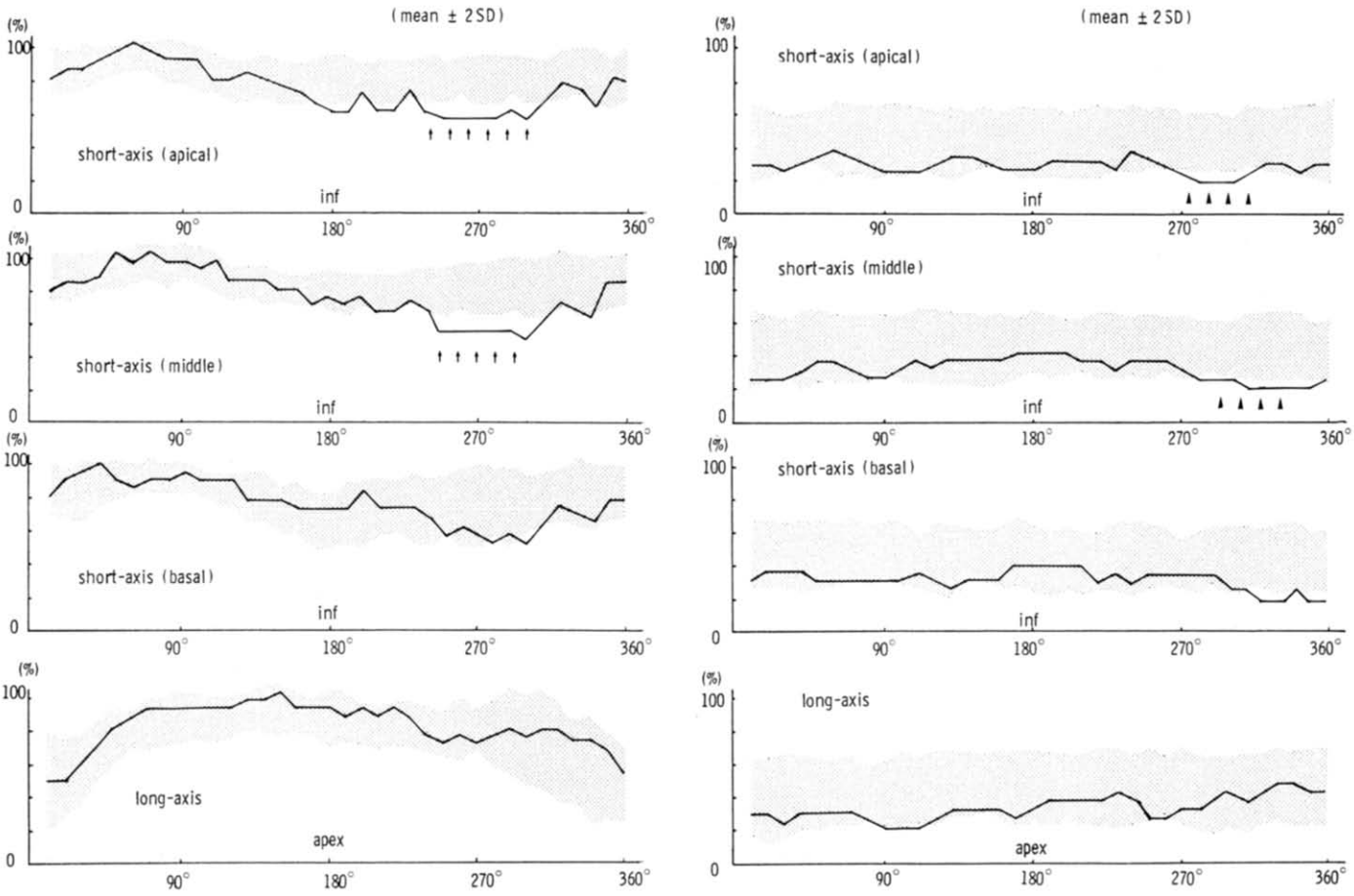

Figure 4. Circumferential profile curves of initial uptake (**left**) and percent washout (**right**) of the same patient (Fig. 3). The initial uptake curves show decreased uptake in the septal region in the short-axis sections (**arrows**). The percent washout curves indicate delayed washout in the same region (**arrowheads**). inf = inferior.

titative analysis of thallium distribution in the myocardium can be done more accurately.

Quantitative analysis of tomographic images. Thallium myocardial distribution is usually interpreted visually in emission tomography (13–17). Although tomographic images seem to be less influenced by observer experience because of higher image contrast than in planar imaging, our study shows that considerable interobserver variability is inevitable. To solve this problem, quantitative analysis is necessary.

Our circumferential profile curves of tomographic images in normal cases indicate that thallium is not uniformly distributed in the left ventricular myocardium. Actually, its distribution in the inferior and septal walls is lower than that in the anterior and lateral walls. This may not necessarily be due to reduced perfusion in the former regions. Instead, photon attenuation and partial volume effect may contribute to such a result (26). Furthermore, normal variation in regional washout should be considered. For these reasons, a precise definition of the lower limit of normal uptake and washout is necessary in quantitative analysis.

In the present study, quantitative tomographic analysis provided better sensitivity for detecting left circumflex artery lesion, especially in patients with multivessel disease. Since thallium distribution in the posterolateral wall is higher than in other regions in normal cases, it may be easier to detect mild perfusion abnormality in this area by comparing the profile curves of normal subjects and those with coronary artery disease.

As for stress planar imaging, several reports (8–11) described a slightly better sensitivity and specificity by quantitative analysis; however, these values were not significantly higher than those obtained by visual interpretation. In addition, increased lung uptake of thallium which is often seen in multivessel disease (25) may impair accurate quantification of thallium distribution by background subtraction. In this respect, emission tomography allows more accurate quantitative analysis because of the full three-dimensional tomographic presentation.

Quantitative tomographic imaging using a seven pinhole collimator (27) did not significantly improve the diagnostic accuracy for diagnosing coronary artery disease as compared with planar imaging. This was consistent with our previous

results (13) in a comparative study of emission transaxial tomography, seven pinhole tomography and planar imaging at rest for detecting myocardial infarction. Limited angle tomography, such as a seven pinhole system, may not necessarily provide accurate tomographic images because of poor depth resolution and artificial defects from malalignment (13,28). In contrast, transaxial emission tomography allows more accurate three-dimensional evaluation of thallium distribution.

Washout analysis as noted in planar imaging (10,11) was also valuable, especially in the evaluation of multivessel disease by emission tomography. Ischemic regions with initial decreased thallium uptake may continue to accumulate thallium or the activity may diminish at a slower rate during the delayed resting stage. In multivessel disease, which may often reveal uniformly decreased thallium distribution, abnormal washout may be detected easier than regional hypoperfusion.

Quantitative criteria for abnormal washout pattern. However, as reported by Becker et al. (29), moderate variation of the washout rate was observed in our normal circumferential profile curves. Therefore, quantitative criteria for an abnormal washout pattern were applied for the assessment of coronary artery disease from the data of the normal profile curves. Actually, the uptake and washout assessed by the normal range profile curves did not decrease the specificity (92 versus 93% for qualitative analysis). One of the difficulties in accurately calculating washout rate in emission tomography is consistent patient positioning. A small point source applied in our study was useful for accurate positioning of the patient. For evaluation of long-axis tomographic sections, the apex was used as a landmark to align in the middle of the circumferential profiles.

Limitations of study. One of the major limitations of thallium emission tomography is the large variation of count statistics because of relatively inadequate count density and large photon attenuation of thallium. Also, the rotating gamma camera device has relatively poor sensitivity as compared with the ring type positron tomography systems. Thus, quantitative evaluation of stress thallium emission tomographic imaging should be done carefully. In this respect, the myocardium was divided into 36 radial segments, instead of the generally utilized 60 radial segments (6,27). Tomographic images were considered abnormal only when values of two or more contiguous radial segments were below the lower limits of normal curves.

Since it takes 16 minutes for tomographic data acquisition, redistribution effects during the acquisition might possibly distort the data. However, this acquisition time appears short enough for evaluation of a transient perfusion abnormality. In contrast, planar imaging performed just after emission tomography can not be comparatively assessed because such a planar method may be handicapped, considering the early redistribution of thallium after exercise (10). Therefore, for comparative evaluation of stress tomography and planar imaging, each method should be performed on different days under approximately the same stress condition (16).

Single photon emission tomography has inherent limitations for absolute quantitation of radionuclide concentration because of inaccurate correction of photon attenuation and scatter (30). To calculate myocardial blood flow, for instance, positron tomography is needed (31). However, relative myocardial perfusion can be assessed by thallium emission tomography in vitro measurement (32), and consequently, it may permit comparative evaluation of regional thallium distribution as well as temporal evaluation of thallium uptake after exercise in a given patient.

Conclusions. This study emphasizes the value of quantitative analysis of stress thallium emission tomography for the evaluation of coronary artery disease. Three-dimensional evaluation of thallium distribution in the myocardium allows an accurate segmental analysis, and consequently, even mildly ischemic regions and deep lesions may be readily detected. Thus, stress emission tomography can provide high diagnostic accuracy for the detection and localization of coronary artery disease.

We gratefully acknowledge Shunichi Tamaki, MD, Yukinoso Suzuki, MD, Ryuji Nohara, MD and Toru Fujita, RT for their valuable cooperation throughout these studies.

References

1. Bailey IK, Griffith LSC, Rouleau J, Strauss HW, Pitt B. Thallium-201 myocardial perfusion imaging at rest and during exercise: comparative sensitivity to electrocardiography in coronary artery disease. Circulation 1977;55:79–87.
2. Ritchie JL, Trobaugh GB, Hamilton GW, et al. Myocardial imaging with thallium-201 at rest and during exercise: comparison with coronary arteriography and resting and stress electrocardiography. Circulation 1977;56:66–71.
3. Hamilton GW, Trobaugh GB, Ritchie JL, Williams DL, Weaver WD, Gould KL. Myocardial imaging with intravenously injected thallium-201 in patients with suspected coronary artery disease: analysis of technique and correlation with electrocardiographic, coronary anatomic and ventriculographic findings. Am J Cardiol 1977;39:347–54.
4. Botvinick EH, Taradash MR, Shames DM, Parmley WW. Thallium-201 myocardial perfusion scintigraphy for the clinical clarification of normal, abnormal and equivocal electrocardiographic stress tests. Am J Cardiol 1978;41:43–59.
5. Trobaugh GB, Wackers FJ, Sokole EB, DeRouen TA, Ritchie JL, Hamilton GW. Thallium-201 myocardial imaging: an interinstitutional study of observer variability. J Nucl Med 1978;19:359–63.
6. Meade RC, Bamrah VS, Horgan JD, Ruetz PP, Kronenwetter C, Yeh EL. Quantitative methods in the evaluation of thallium-201 myocardial perfusion images. J Nucl Med 1978;19:1175–8.
7. Burow RD, Pond M, Schafer AW, Becker L. "Circumferential profiles:" a new method for computer analysis of thallium-201 myocardial perfusion images. J Nucl Med 1979;20:771–81.
8. Watson DD, Campbell NP, Read EK, Gibson RS, Teates CD, Beller GA. Spatial and temporal quantitation of planar thallium myocardial images. J Nucl Med 1981;22:577–84.

9. Berger BC, Watson DD, Taylor GJ, et al. Quantitative thallium-201 exercise scintigraphy for detection of coronary artery disease. J Nucl Med 1981;22:585–93.
10. Garcia E, Maddahi J, Berman D, Waxman A. Space/time quantitation of thallium-201 myocardial scintigraphy. J Nucl Med 1981;22:309–17.
11. Maddahi J, Garcia EV, Berman DS, Waxman A, Swan HJC, Forrester J. Improved noninvasive assessment of coronary artery disease by quantitative analysis of regional stress myocardial distribution and washout of thallium-201. Circulation 1981;64:924–35.
12. Holman BL, Hill TC, Wynne J, Lovett RD, Zimmerman RE, Smith EM Single-photon transaxial emission computed tomography of the heart in normal subjects and in patients with infarction. J Nucl Med 1979;20:736–40.
13. Tamaki N, Mukai T, Ishii Y, et al. Clinical evaluation of thallium-201 emission myocardial tomography using a rotating gamma camera: comparison with seven-pinhole tomography. J Nucl Med 1981;22:849–55.
14. Maublant J, Cassagnes J, LeJeune JJ, et al. A comparison between conventional scintigraphy and emission tomography with thallium-201 in the detection of myocardial infarction. J Nucl Med 1982;23:204–8.
15. Ritchie JL, Williams DL, Harp G, Stratton JL, Caldwell JH. Transaxial tomography with thallium-201 for detecting remote myocardial infarction. Am J Cardiol 1982;50:1236–41.
16. Tamaki N, Yonekura Y, Mukai T, et al. Segmental analysis of stress thallium myocardial emission tomography for localization of coronary artery disease. Eur J Nucl Med 1984;9:99–105.
17. Nohara R, Kambara H, Suzuki Y, et al. Stress scintigraphy using single-photon emission computed tomography (SPECT) in the evaluation of ischemic heart disease. Am J Cardiol 1984;53:1250–4.
18. Tamaki N, Mukai T, Ishii Y, et al. Comparative study of thallium emission myocardial tomography with 180° and 360° data collection. J Nucl Med 1982;23:661–6.
19. Borrello JA, Clinthorne NH, Rogers WL, Thrall HJ, Keyes JW. Oblique-angle tomography: a reconstructing algorithm for transaxial tomographic data. J Nucl Med 1981;22:471–3.
20. Tamaki N, Mukai T, Ishii Y, et al. Multiaxial tomography of heart chambers by gated blood-pool emission computed tomography using a rotating gamma camera. Radiology 1983;147:547–54.
21. Tamaki S, Nakajima H, Murakami T, et al. Estimation of infarct size by myocardial emission computed tomography with thallium-201 and its relation to creatine kinase-MB release after myocardial infarction in man. Circulation 1982;66:994–1001.
22. Tamaki N, Yonekura Y, Kadota K, Kambara H, Chuichi K, Torizuka K. Quantitative analysis of thallium uptake and washout by stress emission computed tomography (ECT) (abstr). Circulation 1983;68(suppl III):III-246.
23. Massie BM, Botvinick EH, Brundage BH. Correlation of thallium-201 scintigrams with coronary anatomy: factors affecting region by region sensitivity. Am J Cardiol 1979;44:616–22.
24. Rigo P, Bailey IK, Griffith LSC, et al. Value and limitations of segmental analysis of stress thallium myocardial imaging for localization of coronary artery disease. Circulation 1980;61:973–81.
25. Kushner FG, Okada RD, Kirshenbaum HD, Boucher CA, Strauss HW, Pohost GM. Lung thallium-201 uptake after stress testing in patients with coronary artery disease. Circulation 1981;63:341–7.
26. Hoffman EJ, Huang SC, Phelps ME. Quantitation in positron emission computed tomography: I. Effect of object size. J Comput Assist Tomogr 1979;3:299–308.
27. Bateman T, Garcia E, Maddahi J, et al. Clinical evaluation of seven-pinhole tomography for the detection and localization of coronary artery disease: comparison with planar imaging using quantitative analysis of myocardial thallium-201 distribution and washout after exercise (abstr). Am Heart J 1983;106:263.
28. Williams DL, Ritchie JL, Harp GD, Caldwell JH, Hamilton GW. In vivo simulation of thallium-201 myocardial scintigraphy by seven-pinhole emission tomography. J Nucl Med 1980;21:821–8.
29. Becker LC, Rogers WJ, Edwards AC. Limitations of thallium washout rate measurements after exercise for detection of coronary artery stenosis (abstr). Circulation 1980;62(suppl III):III-231.
30. Budinger TF. Physical attributes of single-photon tomography. J Nucl Med 1980;21:579–92.
31. Schelbert HR, Phelps ME, Hoffman EJ, Huang S, Selin CE, Kuhl DE. Regional myocardial perfusion assessed with N-13 labeled ammonia and positron emission computerized tomography. Am J Cardiol 1979;43:209–18.
32. Caldwell JH, Williams DL, Hamilton GW, et al. Regional distribution of myocardial blood flow measured by single-photon emission tomography: comparison with in vitro counting. J Nucl Med 1982;23:490–5.